Supporting Information

for publication

Novel cocrystals of 1,2,4-thiadiazole-based potent neuroprotector with carboxylic acids: virtual screening, crystal structures and solubility performance

Artem O. Surov[a], *Alexander P. Voronin*[a], *Nikita A. Vasilev*[a], *Andrey B. Ilyukhin*[b], *German L. Perlovich*[a*]

[a]G.A. Krestov Institute of Solution Chemistry of the Russian Academy of Sciences, 1 Akademicheskaya St., 153045 Ivanovo, Russia;

[b]Institute of General and Inorganic Chemistry RAS, Leninsky Prosp. 31,119991, Moscow, Russia.

*To whom correspondence should be addressed: Telephone: +7-4932-533784; Fax: +7-4932-336237; E-mail glp@isc-ras.ru

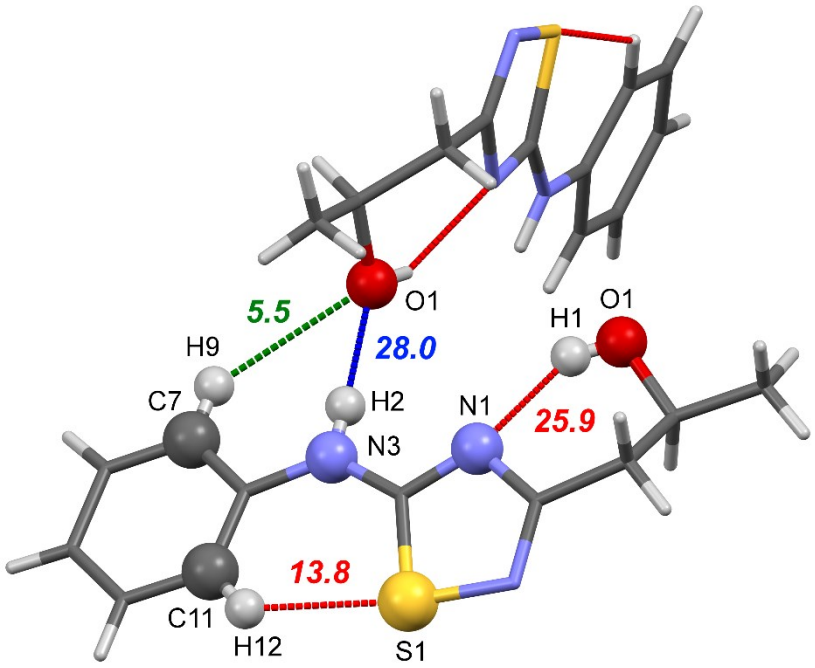

Figure S1. Part of hydrogen-bonded chain in the crystal of pure TDZH (refcode OQOZIF) with shown intramolecular (red dotted lines) and selected intermolecular interactions (blue and green dotted lines). Numbers indicate the energies of selected H-bonds estimated using QTAIMC in kJ·mol^{-1}.

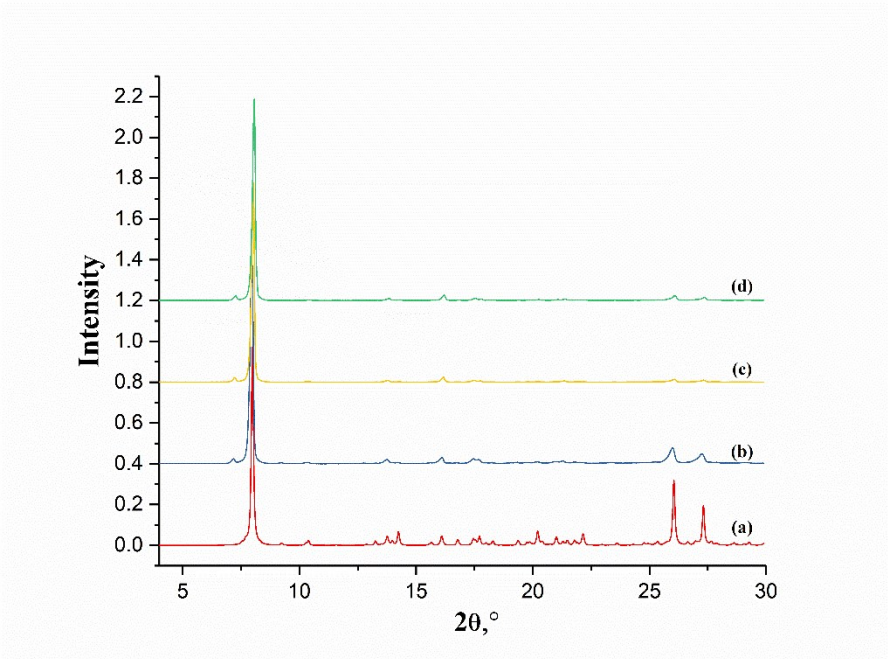

Figure S2. Calculated (a) and experimental PXRD patterns of [**TDZH+VA**] (1:1) obtained via mechanochemical treatment in the presence of methanol (b), acetonitrile (c) and acetonitrile/water mixture(d)

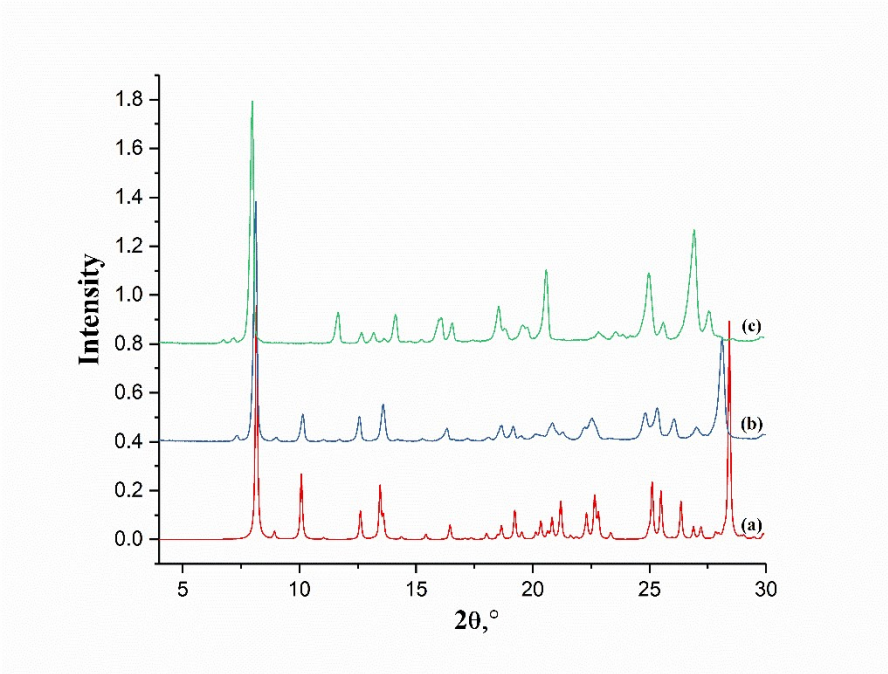

Figure S3. Calculated (a) and experimental PXRD patterns of [**TDZH+GA+H_2O**] obtained via mechanochemical treatment in the presence of acetonitrile/water mixture(b) and neat acetonitrile (c)

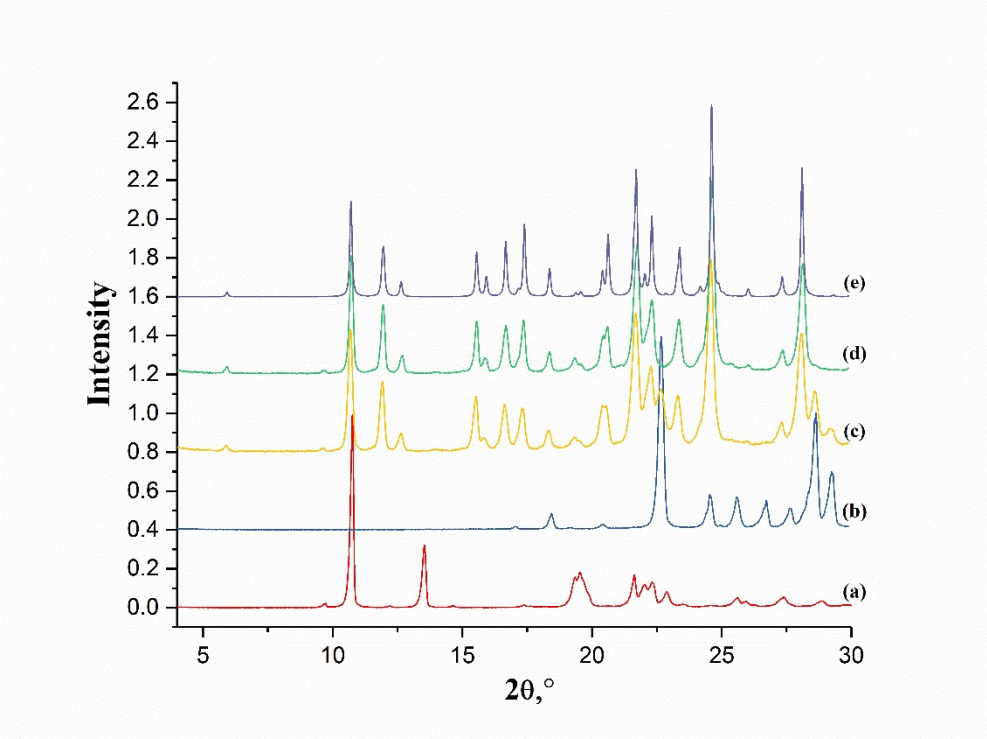

Figure S4. Results of PXRD analyses of parent **TDZH** (a), fumaric acid (b), product of mechanochemical treatment of **TDZH** and fumaric acid in a 1:1 molar ratio (c), product of mechanochemical treatment of **TDZH** and fumaric acid in a 2:1 molar ratio (d), calculated

PXRD patterns of the [**TDZH**+**FumAc**] (2:1) cocrystal (e).

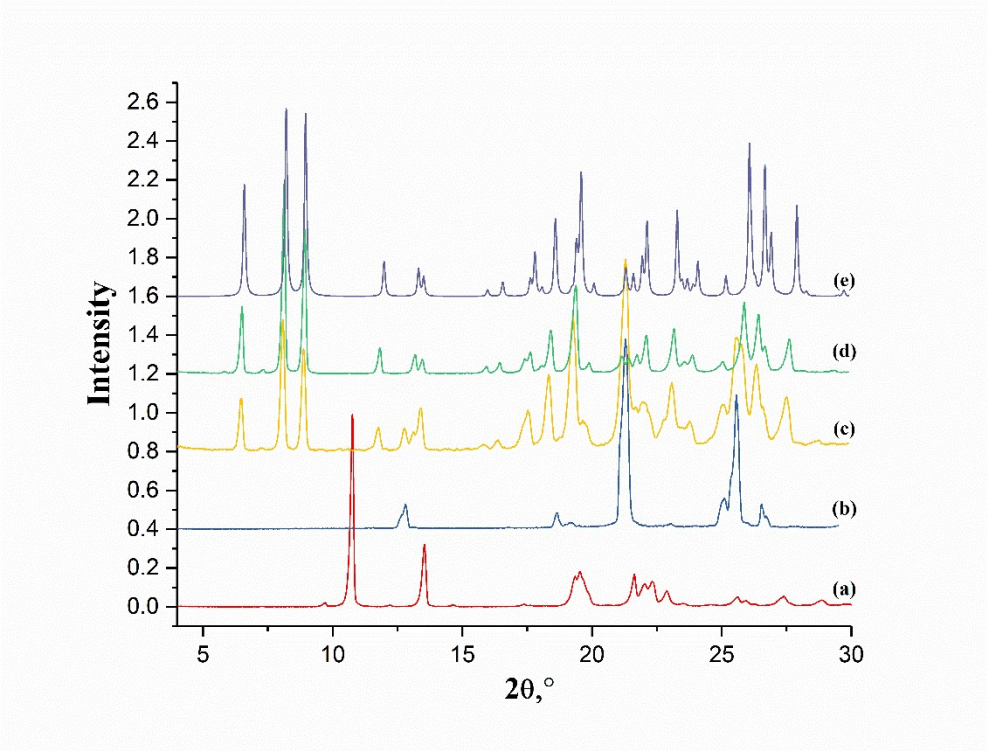

Figure S5. Results of PXRD analyses of parent **TDZH** (a), adipic acid (b), product of mechanochemical treatment of **TDZH** and adipic acid in a 1:1 molar ratio (c), product of mechanochemical treatment of **TDZH** and adipic acid in a 2:1 molar ratio (d), calculated PXRD patterns of the [**TDZH**+**AdipAc**] (2:1) cocrystal (e).

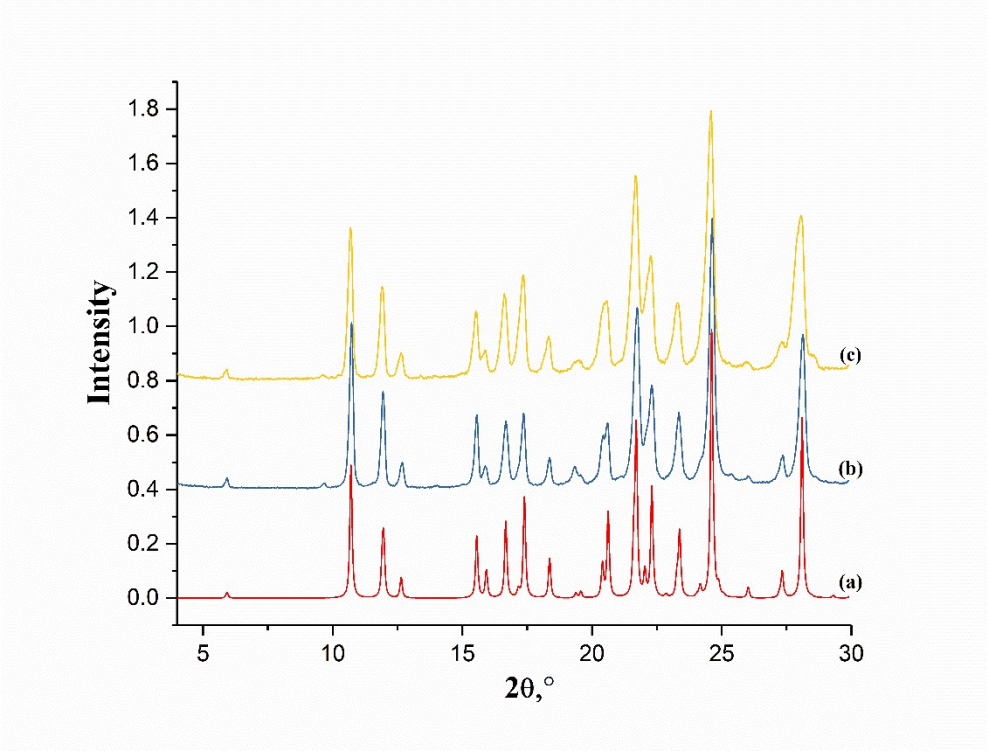

Figure S6. Calculated PXRD patterns of [**TDZH**+**FumAc**] (2:1) (a), experimental PXRD of product of mechanochemical treatment of **TDZH** with fumaric acid (b) and maleic acid (c) in a 2:1 molar ratio

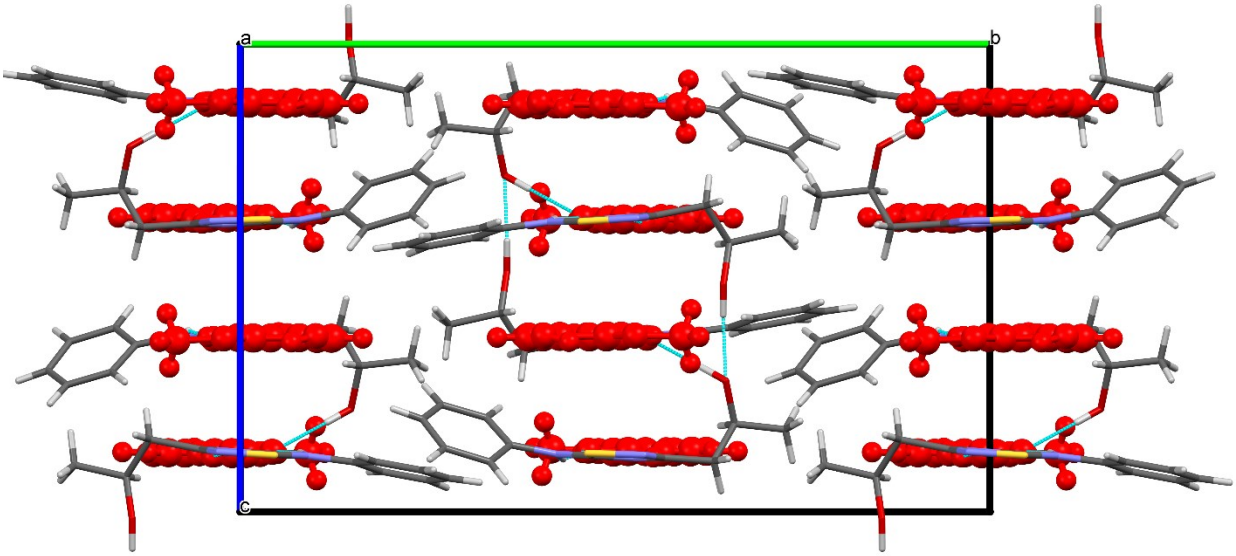

Figure S7. Packing projection of [**TDZH+VA**] (1:1) cocrystal along the ***a*** axis. Coformer molecules are shown in ball and stick and colored red.

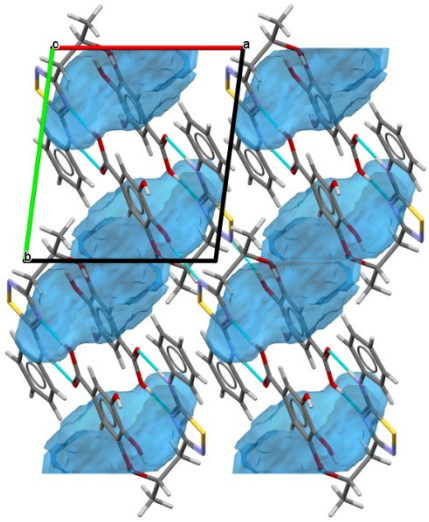

Figure S8. Packing arrangement and void maps in the crystal structures of the [**TDZH+GA+H_2O**] (1:1:2.5) cocrystal.

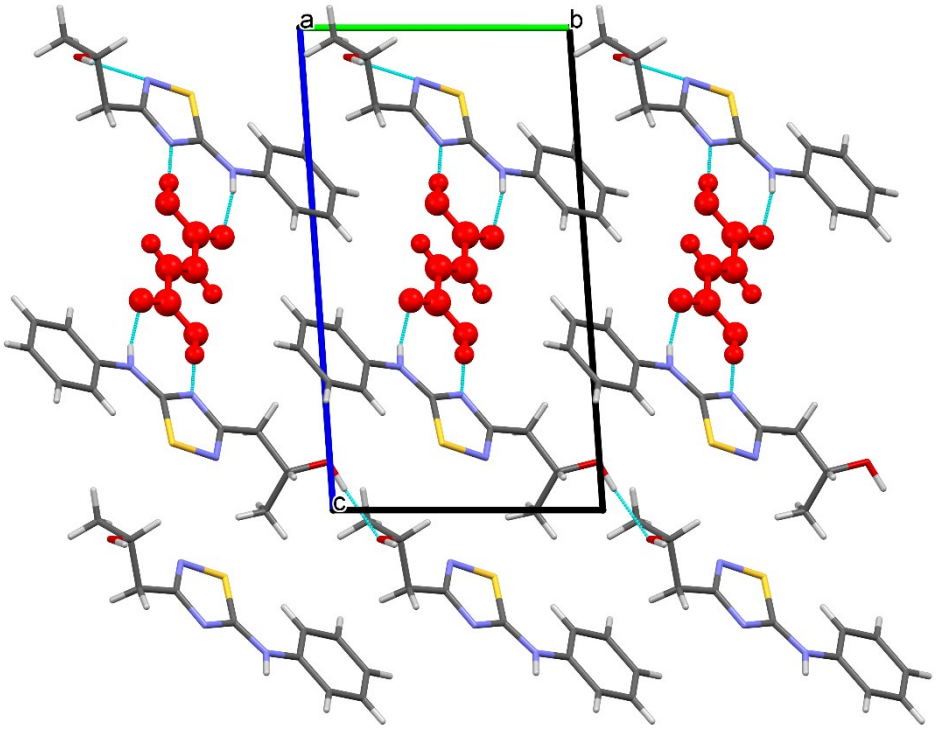

Figure S9. Packing projection of [**TDZH+FumAc]** (2:1) cocrystal along the ***a*** axis. Coformer molecules are shown in ball and stick and colored red.

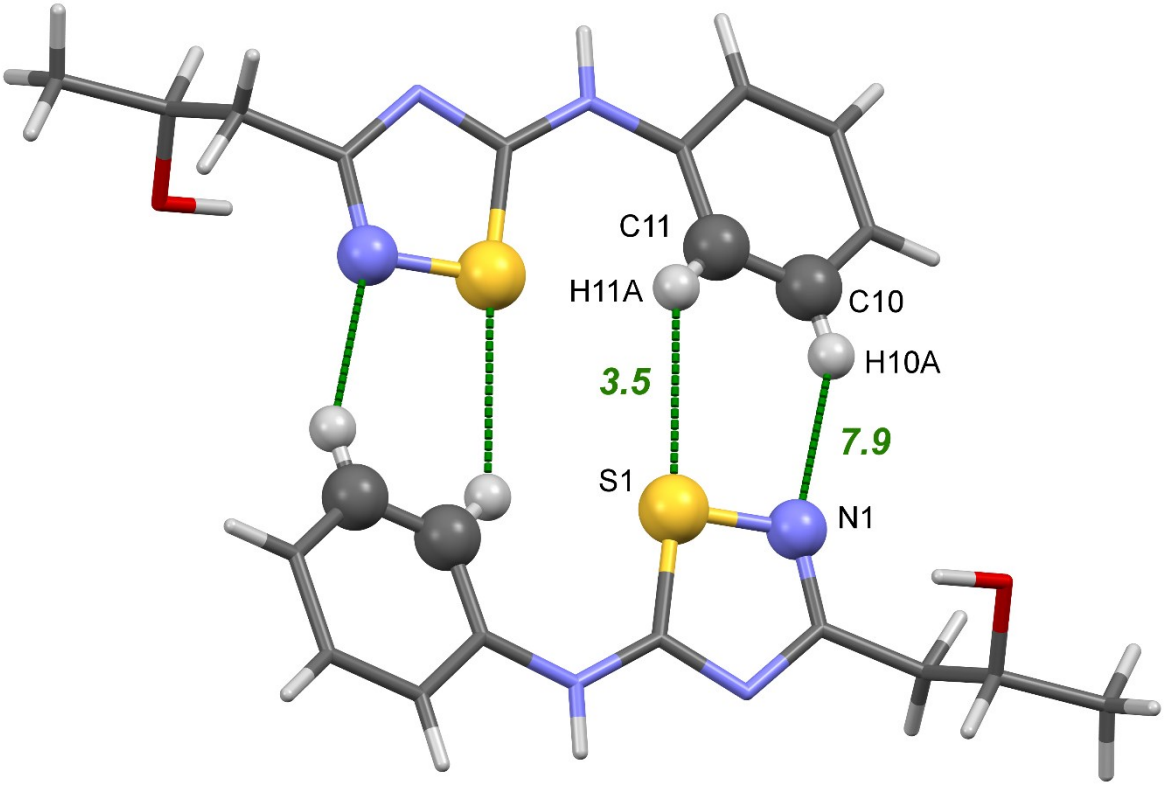

Figure S10. A centrosymmetric dimer of TDZH in the [**TDZH+AdipAc]** (2:1) crystal held by two non-conventional hydrogen bonds (shown as green dotted lines). Numbers indicate the energies of selected interactions estimated using QTAIMC in kJ·mol^{-1}.

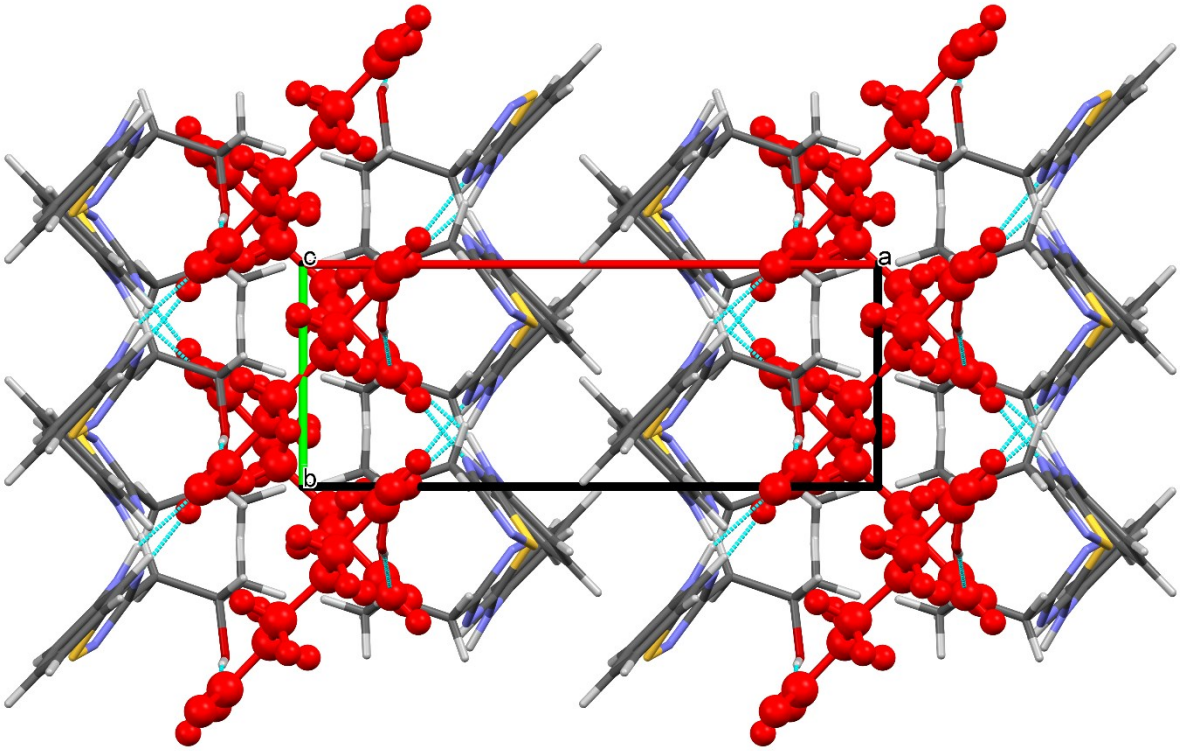

Figure S11. Packing projection of [**TDZH+AdipAc**] (2:1) cocrystal along the ***c*** axis. Coformer molecules are shown in ball and stick and colored red.

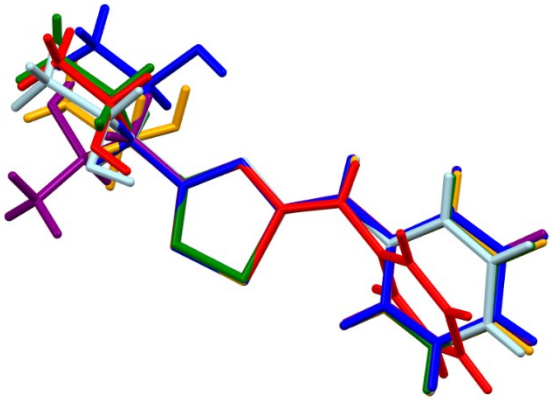

Figure S12. Overlay of TDZH conformations in crystals of parent **TDZH** (blue), [**TDZH+FumAc]** (2:1) (purple), [**TDZH+GA+H_2O]** (1:1:2.5) (orange), [**TDZH+AdipAc]** (2:1) (light blue), [**TDZH+VA]** (1:1) (green), and [**TDZH+OxalAc]** (2:1) (red).

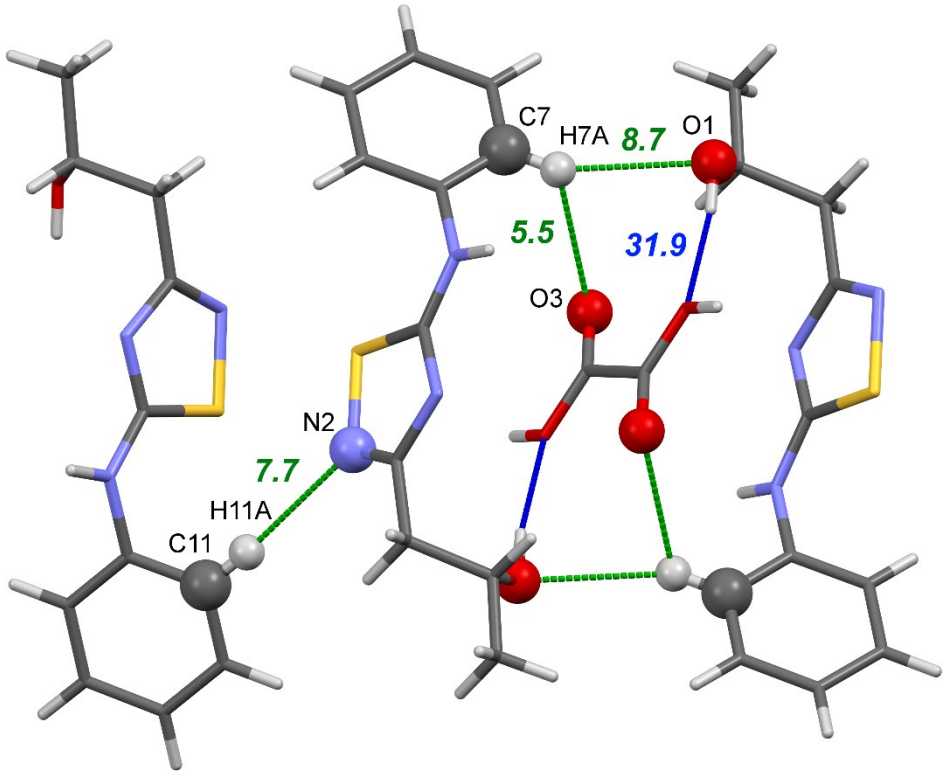

Figure S13. Part of crystal structure of [**TDZH+OxalAc]** (2:1) showing notable hydrogen bonds of phenyl C-H groups with nearby acceptors (green dotted lines) and side O-H…O bond between TDZH and OxalAc molecules (blue dotted line). Numbers indicate the energies of selected interactions estimated using QTAIMC in kJ·mol^{-1}.

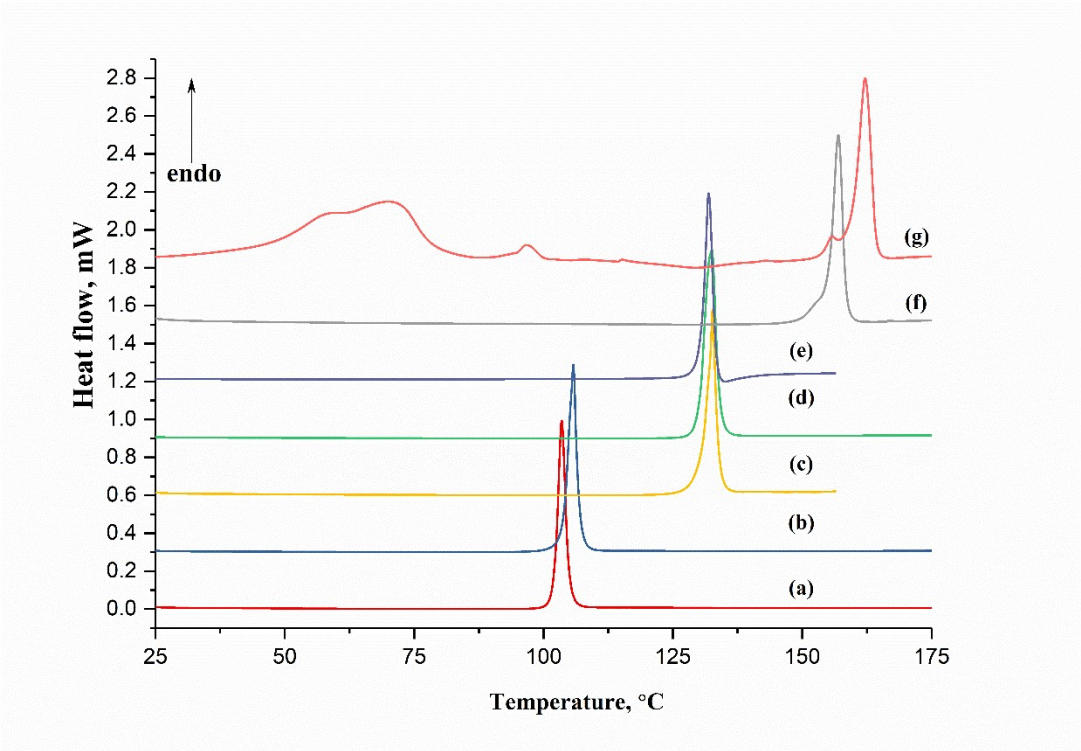

Figure S14. Experimental DSC curves of initial **TDZH** (a), [**TDZH+AdipAc]** (2:1) (b),

[**TDZH+OxalAc]** (2:1) (c), [**TDZH+FumAc]** (2:1) (d), [**TDZH+VA]** (1:1) (e), anhydrous [**TDZH+GA]** (1:1) (f) and [**TDZH+GA+H_2O]** (1:1:2.5) (g)

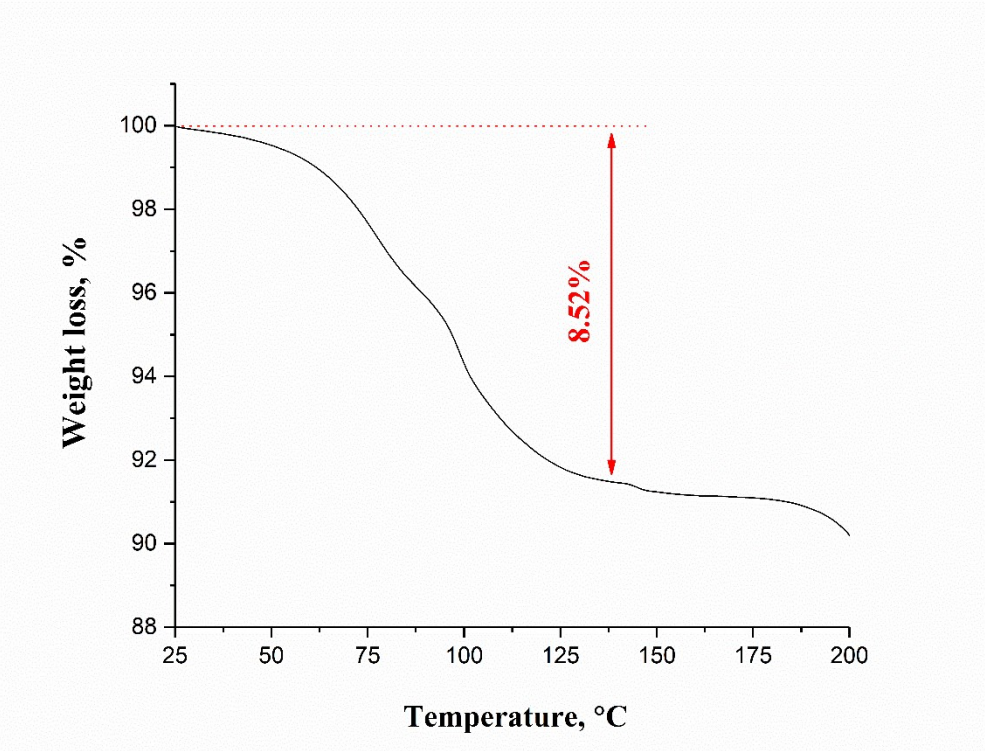

Figure S15. Results of TG analyses of [**TDZH+GA+H_2O]** (1:1:2.5)

Table S1. Calculated change in interaction site pairing energies (ΔE in kJ·mol^{-1}) for the TDZH+coformer systems assuming 1:1 molar ratio and results of experimental co-crystal screening

	ΔE[a]	ΔE_{cr}[b]	Exp. outcome
TDZH+OxalAc	-1.8	-4.2	[**TDZH+OxalAc]** (2:1)
TDZH+FumAc	-1.4	-0.2	[**TDZH+FumAc]** (2:1)
TDZH+MaleicAc	5.1	-	[**TDZH+FumAc]** (2:1)
TDZH+AdipAc	-0.1	-1.0	[**TDZH+AdipAc]** (2:1)
TDZH+VA	-1.0	-2.9	[**TDZH+VA]** (1:1)
TDZH+GA	-2.5	-3.9	[**TDZH+GA+H_2O]** (1:1:2.5)

[a]Calculated according to procedure described in the 2.10 section of the Materials and Methods part using geometry optimized coformer molecules and a particular conformation of TDZH

[b]Calculated using the molecular conformations of TDZH and coformers extracted directly from the crystal structures of the obtained cocrystals

Table S2. Crystallographic data for multicomponent crystals of TDZH with carboxylic acids

	[**TDZH+VA**] (1:1)	[**TDZH+GA+ H_2O**] (1:1:2.5)	[**TDZH+OxAc**] (2:1)	[**TDZH+AdipAc**] (2:1)	[**TDZH+FumAc**] (2:1)
Crystal data					
Chemical formula	$C_{11}H_{13}N_3OS \cdot C_8H_8O_4$	$C_{11}H_{13}N_3OS \cdot C_7H_6O_5 \cdot 2.5(H_2O)$	$C_{11}H_{13}N_3OS \cdot 0.5(C_2H_2O_4)$	$C_{11}H_{13}N_3OS \cdot 0.5(C_6H_{10}O_4)$	$C_{11}H_{13}N_3OS \cdot 0.5(C_4H_4O_4)$
M_r	403.45	450.46	280.32	308.37	293.34
Crystal system	Monoclinic	Triclinic	Monoclinic	Monoclinic	Triclinic
Space group	$P2_1/n$	$P\bar{1}$	$P2_1/n$	$P2_1/c$	$P\bar{1}$
Temperature (K)	150	150	150	150	296
a (Å)	13.4199(5)	9.5188 (12)	14.3570 (19)	13.770 (2)	5.7508 (1)
b (Å)	21.9195(10)	9.9520 (12)	4.8081 (5)	5.0916 (4)	8.5166 (2)
c (Å)	13.5946(6)	11.8041 (15)	20.166 (3)	22.201 (2)	14.7464 (3)
α (°)	90	97.589 (4	90	90	84.878 (1)
β (°)	101.160(3)	113.069 (4)	103.286 (10)	106.637 (9)	85.115 (1)
γ (°)	90	93.795 (4)	90	90	74.344 (1)
V (Å^3)	3923.3(3)	1011.2 (2)	1354.8 (3)	1491.4 (3)	691.26 (2)
Z	8	2	4	4	2
Radiation type	Cu $K\alpha$	Mo $K\alpha$	Cu $K\alpha$	Cu $K\alpha$	Cu $K\alpha$
μ (mm^{-1})	1.78	0.22	2.21	2.06	2.19
Crystal size (mm)	0.30 × 0.32 ×0.06	0.28 × 0.24 × 0.18	0.2 × 0.08 × 0.01	0.16 × 0.12 × 0.04	0.3 × 0.2 × 0.08
Data collection					
Diffractometer	Bruker AXS D8 VENTURE PHOTON III C14 IuS 3.0	Bruker *APEX3* CCD	Bruker AXS D8 VENTURE PHOTON III C14 IuS 3.0	Bruker AXS D8 VENTURE PHOTON III C14 IuS 3.0	Bruker AXS D8 VENTURE PHOTON III C14 IuS 3.0
T_{min}, T_{max}	0.7533, 0.4156	0.664, 0.746	0.356, 0.752	0.402, 0.753	0.496, 0.754
Reflns. measured	30859	11729	8414	12113	10893
Independent reflns.	7358	3973	2128	2593	2831
observed reflns. with[$I > 2\sigma(I)$]	5736	3289	1241	2344	2643
R_{int}	0.067	0.036	0.102	0.060	0.029
$(\sin\theta/\lambda)_{max}$ (Å^{-1})	0.615	0.617	0.578	0.601	0.636
Refinement					
$R[F^2 > 2\sigma(F^2)]$, $wR(F^2)$, S	0.075, 0.19, 0.96	0.062, 0.14, 1.18	0.085, 0.208, 0.99	0.043, 0.129, 0.95	0.037, 0.106, 0.98
No. of reflections	7358	3973	2128	2593	2831
No. of parameters	537	295	172	219	210
No. of restraints	35	0	0	44	0
$\Delta\rangle_{max}$, $\Delta\rangle_{min}$ (e Å^{-3})	0.769, -0.722	0.623, -0.364	0.56, -0.38	0.44, -0.27	0.19, -0.37

Table S3. Contributions of different types of non-covalent interactions into the lattice energies of studied multicomponent crystals of TDZH estimated by QTAIMC[a]

	[**TDZH+VA**] (1:1)[b]	[**TDZH+GA+ H_2O**] (1:1:2.5)	[**TDZH+OxAc**] (2:1)	[**TDZH+AdipAc**] (2:1)	[**TDZH+FumAc**] (2:1)
E_{latt}	248.4	477.2	238.5	206.7	196.7
Σ*E* (X-H···X)	129.0 (51.9%)	330.1 (69.2%)	137.9 (57.8%)	94.3 (45.6%)	104.5 (53.1%)
Σ*E* (C–H···X)	51.8 (20.9%)	56.8 (11.9%)	49.7 (20.8%)	59.9 (29%)	47.5 (24.2%)
Σ*E* (C–H···π)	14.3 (5.8%)	4.1 (0.9%)	7.3 (3.1%)	12.2 (5.9%)	5.5 (2.8%)
Σ*E* (π···π)	35.6 (14.3%)	71.7 (15%)	28 (11.8%)	26.2 (12.7%)	28.8 (14.6%)
Other	17.7 (7.1%)	14.4 (3%)	15.6 (6.5%)	14.2 (6.9%)	10.3 (5.2%)
TDZH-CF	200.7 (80.8%)	190.4 (39.9%)	170.6 (71.5%)	119.4 (57.7%)	104.8 (53.3%)
TDZH-TDZH	37.5 (15.1%)	34.5 (7.2%)	63.6 (26.7%)	77.8 (37.6%)	85 (43.2%)
CF-CF	10.2 (4.1%)	20.9 (4.4%)	4.3 (1.8%)	9.6 (4.7%)	6.8 (3.5%)
TDZH-H_2O	–	59.8 (12.5%)	–	–	–
CF-H_2O	–	115.0 (24.1%)	–	–	–
H_2O-H_2O	–	56.5 (11.8%)	–	–	–

[a] All values are given in kJ·mol^{-1} per asymmetric unit (except [**TDZH+VA**] (1:1), see below) and % of the E_{latt} value.

[b] For [**TDZH+VA**] (1:1), all value are given per half of the asymmetric unit (1 molecule of TDZH and 1 molecule of VA)

Table S4. Experimental solubility (S_{CC}) of TDZH cocrystals at the equilibrium pH and 25.0°C, solubility advantage (SA), eutectic constants (K_{eu}) and K_{sp} values

Cocrystal	pH_{eq}	$[TDZH]_{eu}$, $mol \cdot l^{-1}$	$[CF]_{eu}$, $mol \cdot l^{-1}$	S_{cc}, $mol \cdot l^{-1}$
[TDZH+VA] (1:1)	2.3	$(4.4\pm0.5)\cdot10^{-3}$	$(1.8\pm0.3)\cdot10^{-3}$	$(2.8\pm0.4)\cdot10^{-3}$
	3.2	$(3.9\pm0.5)\cdot10^{-3}$	$(1.3\pm0.4)\cdot10^{-3}$	$(2.3\pm0.5)\cdot10^{-3}$
[TDZH+GA+H2O]	2.2	$(4.6\pm0.4)\cdot10^{-3}$	$(7.3\pm0.4)\cdot10^{-3}$	$(5.8\pm0.4)\cdot10^{-3}$
(1:1:2.5)	3.2	$(3.8\pm0.5)\cdot10^{-3}$	$(7.5\pm0.5)\cdot10^{-3}$	$(5.3\pm0.5)\cdot10^{-3}$
[TDZH+Fum]	2.0	$(4.6\pm0.5)\cdot10^{-3}$	$(1.8\pm0.3)\cdot10^{-3}$	$(4.3\pm0.5)\cdot10^{-3}$
(2:1)	2.7	$(4.0\pm0.6)\cdot10^{-3}$	$(1.5\pm0.4)\cdot10^{-3}$	$(3.7\pm0.6)\cdot10^{-3}$
[TDZH+Adip]	2.1	$(4.0\pm0.4)\cdot10^{-3}$	$(1.0\pm0.1)\cdot10^{-2}$	$(7.0\pm0.6)\cdot10^{-3}$
(2:1)	4.9	$(3.6\pm0.4)\cdot10^{-3}$	$(3.9\pm0.2)\cdot10^{-2}$	$(9.9\pm0.8)\cdot10^{-3}$
[TDZH+Oxal] (2:1)	1.2	$(8.6\pm0.8)\cdot10^{-3}$	$(1.0\pm0.3)\cdot10^{-2}$	$(2.5\pm0.3)\cdot10^{-2}$